

Solvothermal syntheses and crystal structures of two new thiogermanates $[M(dap)_3]_4Ge_4S_{10}Cl_4$ ($M = Co, Ni$) with metal complexes as counterions

Feng Zhang · Xing Liu · Jian Zhou ·
Xian-Hong Yin · Jun He

Received: 24 November 2010 / Accepted: 3 May 2011 / Published online: 7 June 2011
© Springer-Verlag 2011

Abstract Two new transition-metal thiogermanates $[M(dap)_3]_4Ge_4S_{10}Cl_4$ ($M = Co, Ni$; dap = 1,2-propanediamine) have been solvothermally synthesized and structurally characterized. The two thiogermanates are isostructural and consist of discrete $Ge_4S_{10}^{4-}$ adamantane-like ions, free Cl^- ions, and $[M(dap)_3]^{2+}$ cations as counterions. The $Ge_4S_{10}^{4-}$ anion is built from corner-sharing connection of four GeS_4^{4-} tetrahedra. Although some chalcogenidogermanates have been obtained by use of in situ generated transition-metal complexes as structure-directing agents under mild solvothermal conditions, their anions are usually dimeric $[Ge_2Q_6]^{4-}$ ($Q = S, Se$) species. The new thiogermanates are rare examples of adamantane-like ($Ge_4S_{10}^{4-}$) thiogermanates combined with transition-metal complexes. Their optical properties have been investigated by UV–Vis spectra.

Keywords Solvothermal synthesis · Crystal structure · Thiogermanates · Metal complexes

Introduction

Research involving new chalcogenogermanates has attracted much attention since 1989, because of their rich structural diversity and potential applications in gas separation, nonlinear optical, and ferroelectric and thermoelectric materials [1–4]. In the case of thiogermanates, a lot of extended microporous thiogermanates have been synthesized by mild hydrothermal methods in the presence of tetraalkylammonium hydroxides or nonchelating amines to date [5–10]. Their structures are generally constructed by the linkage of a $[Ge_4S_{10}]^{4-}$ adamantane-like unit and MS_x polyhedron ($M =$ transition-metal ions). Protonated nonchelating amines or tetraalkylammonium ions as structure-directing agents are commonly retained within pore or cavity spaces. Recently, there has been considerable interest in use of metal complexes instead of organic amines or tetraalkylammonium ions as structure-directing agents in making metal chalcogenides under hydro- or solvothermal conditions, because some of them are chiral complexes, which can transfer the chirality to the polymeric frameworks [11–13]. So far, a number of thioantimonates have been made, as exemplified by $[M(en)_3][Sb_4S_7]$ ($M = Fe, Co, Ni$) [14, 15], $[Co(en)_3][Sb_{12}S_{19}]$ [16], $[Co(en)_3]CoSb_4S_8$ [17], $[Fe(dien)_2]Sb_4S_7 \cdot H_2O$ [18], $[Co(dien)_2]Sb_4S_7 \cdot 0.5H_2O$ [18], $[Ni(dien)-(tren)]Sb_4S_7$ [18], $[Fe(tren)]FeSb_4S_4$ [19], $[Fe(dien)_2]Fe_2Sb_4S_{10}$ [19], and $[Ni(dien)_2]_3(Sb_3S_6)_2$ [20]. However, compared with the thioantimonates, thiogermanates with metal complexes are less explored under mild solvothermal conditions; the limited examples include $[M(en)_3]_2Ge_2S_6$ ($M = Mn, Ni$) [21], $\{[M(tepa)]_2(\mu-Ge_2S_6)\}$ ($M = Mn, Co, Ni$) [22, 23], $[Ni(dien)_2]_2(Ge_2S_6)$ [23], $[Ni(dien)_2](H_2\text{pipe}) (Ge_2S_6)$ [23], and $\{[Mn(tren)]_2(\mu_2-Ge_2S_6)\}$ [23]. Their anions are usually dimeric $[Ge_2S_6]^{4-}$ species, but isolated $Ge_4S_{10}^{4-}$ adamantane-like anions with metal complex cations as counterions are

F. Zhang · J. Zhou (✉) · X.-H. Yin (✉)
College of Chemistry and Ecological Engineering,
Guangxi University for Nationalities, Nanning 530006,
People's Republic of China
e-mail: jianzhou888888@163.com

X.-H. Yin
e-mail: 6628yxh@163.com

X. Liu · J. Zhou · J. He
Department of Chemistry and Biology,
Yulin Normal University, Yulin 537000,
People's Republic of China

relatively rare. Herein, we report the syntheses and structures of two new transition-metal thiogermanates $[M(\text{dap})_3]_4\text{Ge}_4\text{S}_{10}\text{Cl}_4$ [$M = \text{Co}$ (**1**), Ni (**2**); $\text{dap} = 1,2\text{-propanediamine}$]. **1** and **2** are rare examples of $\text{Ge}_4\text{S}_{10}^{4-}$ adamantane-like anions with metal complex cations.

Results and discussion

Both **1** and **2** were synthesized by direct reaction of GeO_2 , Sb , S , and $\text{MCl}_2 \cdot 6\text{H}_2\text{O}$ ($M = \text{Co}, \text{Ni}$) in dap solution at 165°C . Although Sb in **1** and **2** was not incorporated into the final structures, Sb was found to enhance the crystal growth of **1** and **2**, which played an important role in the formation of $\text{Ge}_4\text{S}_{10}^{4-}$ adamantane-like ions. When the above reaction system reacted in the absence of Sb , only a gray amorphous product was obtained. **1** and **2** are isostructural and crystallize in the tetragonal space group $I4_12_2$. Their structures consist of discrete $[\text{Ge}_4\text{S}_{10}]^{4-}$ adamantane-like ions, $[\text{M}(\text{dap})_3]^{2+}$ ions, and Cl^- ions (Fig. 1a). In **1** and **2**, the $[\text{Ge}_4\text{S}_{10}]^{4-}$ adamantane-like anion is formed by four edge-sharing GeS_4 tetrahedra. Some important bond lengths for **1** and **2** are listed in Table 1. The $\text{Ge}-\text{S}_t$ distances [2.1130(13)–2.1147(16) Å, $t = \text{terminal}$] are shorter than those of the bridging $\text{Ge}-\text{S}_b$ bond [2.2209(14)–2.2420(13) Å, $b = \text{bridging}$]. Distorted GeS_4 tetrahedra are demonstrated by the $\text{S}-\text{Ge}-\text{S}$ angles [105.58(6)–112.24(3)°] deviating from the

ideal value of 109.5° . These adamantane $[\text{Ge}_4\text{S}_{10}]^{4-}$ ions are not linked to each other and are arranged in a trigonal manner along the a -axis (Fig. 1b). The trigonal manners always occur in pairs with a center of inversion. The average distance between the centers of two neighboring triangles is close to 10.8 Å. Two inverse triangles form a pseudodimeric unit, which forms a planar array of approximate hexagonal packing, every pseudodimeric unit being surrounded by six neighbors (Table 1).

Each M^{2+} ion is coordinated by six N atoms of three dap ligands forming octahedra. The $[\text{Co}(\text{dap})_3]^{2+}$ and $[\text{Ni}(\text{dap})_3]^{2+}$ cations are distorted octahedra with octahedral axial $\text{N}-\text{Co}-\text{N}$ and $\text{N}-\text{Ni}-\text{N}$ angles ranging from $168.0(3)^\circ$ to $174.7(2)^\circ$ and $168.3(3)^\circ$ to $174.6(3)^\circ$, respectively. The $\text{Co}-\text{N}$ and $\text{Ni}-\text{N}$ bond distances in the range from 2.110(5) to 2.134(5) Å and 2.109(6) to 2.148(5) Å, respectively, are comparable to those in other $[\text{M}(\text{dap})_3]^{2+}$ or $[\text{M}(\text{en})_3]^{2+}$ cations [14, 15, 24].

Intensive H-bonding interactions appear to be a key factor in the stabilization of extended structure in **1**. The adjacent $[\text{Co}(\text{dap})_3]^{2+}$ cations are linked into a one-dimensional (1-D) zigzag chain by way of $\text{N}2-\text{H}2\text{B}\dots\text{Cl}2$ H-bonds, running parallel to the b -axis. Another straight chain is built from the combination of $\text{N}5-\text{H}5\text{A}\dots\text{Cl}1$ and $\text{N}7-\text{H}7\text{A}\dots\text{Cl}1$ H-bonds. Two types of chains are alternately arranged along the a -axis and are connected via $\text{N}1-\text{H}1\text{B}\dots\text{Cl}1$ H-bonds, forming a layered arrangement parallel to the (001) plane (Fig. 2). Then, the layers interact also via $\text{N}6-\text{H}6\text{A}\dots\text{Cl}2$ H-bonds, resulting in a three-dimensional (3-D) network structure (Fig. 3). The S atoms of $[\text{Ge}_4\text{S}_{10}]^{4-}$ anions form H-bonding interactions with the NH_2^- groups of the neighboring $[\text{Co}(\text{dap})_3]^{2+}$ cations, which fix $[\text{Ge}_4\text{S}_{10}]^{4-}$ anions within 3-D network. Similar $\text{N}-\text{H}\dots\text{Cl}$ and $\text{N}-\text{H}\dots\text{S}$ H-bonds are observed in **2** (Table 2).

UV-Vis absorption spectra of **1** and **2** were calculated from the data of diffuse reflectance by using the Kubelka-Munk function (Fig. 4). The weak absorptions at 2.63 eV in **1**, and 1.38 eV and 2.31 eV in **2** presumably arise from d-d electronic transition of previously reported molecular $\text{Co}^{2+}/\text{Ni}^{2+}$ complexes [25]. The optical band gaps (E_{onset}) obtained by extrapolation of the linear portion of the absorption edges are estimated to be 3.21 eV for **1** and 3.31 eV for **2**, which can be assigned to the lowest possible electronic excitation located at the $[\text{Ge}_4\text{S}_{10}]^{4-}$ anion. The values are very close to those of $[\text{Ge}_3\text{S}_6\text{Zn}(\text{H}_2\text{O})\text{S}_3\text{Zn}(\text{H}_2\text{O})][(\text{Zn}(\text{tren})(\text{H}_2\text{O})]$ (3.4 eV) [26] and $\text{Rb}_3(\text{AlS}_2)_3(\text{GeS}_2)_7$ (3.1 eV) [27], which exhibit the properties of a wide-band-gap semiconductor. The thermogravimetric (TG) behavior of **1** and **2** was investigated (Fig. 5). Their TG curves show that similar one-step weight losses (47.16% for **1** and 47.25% for **2**) occur in the range of 100–600 °C, assigned to the removal of the dap ligand (calc. 47.02%).

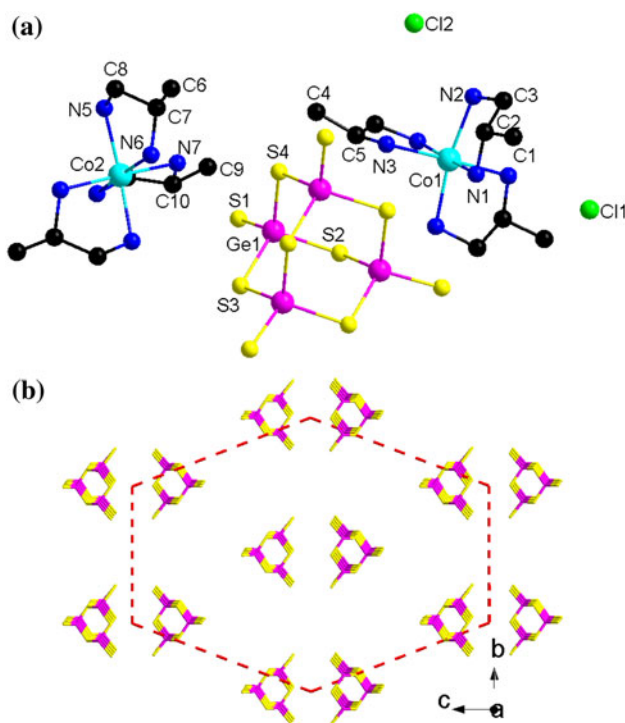


Fig. 1 (a) Crystal structure of **1** (all H atoms omitted for clarity). (b) The packing of the $[\text{Ge}_4\text{S}_{10}]^{4-}$ ions

Table 1 Selected bond distances (\AA) and angles ($^\circ$) for **1** and **2**

1			
Ge1-S1	2.1130(13)	Ge1-S2	2.2349(11)
Ge1-S3	2.2420(13)	Ge1-S4	2.2209(14)
Co1-N1	2.122(5)	Co1-N2	2.125(5)
Co1-N3	2.124(6)	Co2-N5	2.117(5)
Co2-N6	2.110(5)	Co2-N7	2.134(5)
S1-Ge1-S4	111.72(8)	S1-Ge1-S2	105.58(6)
S4-Ge1-S2	109.94(4)	S1-Ge1-S3	108.47(9)
S4-Ge1-S3	112.24(3)	S2-Ge1-S3	108.63(4)
N1-Co1-N1#1	91.2(3)	N1-Co1-N3#1	174.7(2)
N1#1-Co1-N3#1	93.8(2)	N1-Co1-N3	93.8(2)
N1#1-Co1-N3	174.7(2)	N3#1-Co1-N3	81.4(4)
N1-Co1-N2	82.04(19)	N1#1-Co1-N2	90.9(2)
N3#1-Co1-N2	95.9(2)	N3-Co1-N2	91.8(2)
N1-Co1-N2#1	90.9(2)	N1#1-Co1-N2#1	82.04(19)
N3#1-Co1-N2#1	91.8(2)	N3-Co1-N2#1	95.9(2)
N2-Co1-N2#1	169.9(3)	N6#2-Co2-N6	94.3(3)
N6#2-Co2-N5	91.11(18)	N6-Co2-N5	80.72(18)
N6#2-Co2-N5#2	80.72(18)	N6-Co2-N5#2	91.11(18)
N5-Co2-N5#2	168.0(3)	N6#2-Co2-N7	172.8(2)
N6-Co2-N7	92.96(19)	N5-Co2-N7	90.3(2)
N5#2-Co2-N7	99.0(2)	N6#2-Co2-N7#2	92.96(19)
N6-Co2-N7#2	172.8(2)	N5-Co2-N7#2	99.0(2)
N5#2-Co2-N7#2	90.3(2)	N7-Co2-N7#2	79.8(3)
2			
Ge1-S1	2.2267(13)	Ge1-S2	2.1147(16)
Ge1-S3	2.2382(17)	Ge1-S4	2.2284(19)
Ni1-N1	2.115(5)	Ni1-N2	2.121(5)
Ni1-N3	2.148(5)	Ni2-N4	2.109(6)
Ni2-N6	2.123(7)	Ni2-N5	2.130(5)
S2-Ge1-S1	105.71(7)	S2-Ge1-S4	111.24(10)
S1-Ge1-S4	110.20(4)	S2-Ge1-S3	108.66(10)
S1-Ge1-S3	108.83(4)	S4-Ge1-S3	111.97(4)
N1#3-Ni1-N1	168.3(3)	N1#3-Ni1-N2	90.9(2)
N1-Ni1-N2	81.1(2)	N1#3-Ni1-N2#3	81.1(2)
N1-Ni1-N2#3	90.9(2)	N2-Ni1-N2#3	94.2(3)
N1#3-Ni1-N3#3	98.5(2)	N1-Ni1-N3#3	90.5(2)
N2-Ni1-N3#3	93.2(2)	N2#3-Ni1-N3#3	172.6(2)
N1#3-Ni1-N3	90.5(2)	N1-Ni1-N3	98.5(2)
N2-Ni1-N3	172.6(2)	N2#3-Ni1-N3	93.2(2)
N3#3-Ni1-N3	79.4(3)	N4#4-Ni2-N3	170.0(3)
N4#4-Ni2-N6#4	95.8(2)	N4-Ni2-N6#4	91.8(2)
N4#4-Ni2-N6	91.8(2)	N4-Ni2-N6	95.8(2)
N6#5-Ni2-N6	81.1(4)	N4#4-Ni2-N5#4	81.8(2)
N4-Ni2-N5#4	91.2(2)	N6#4-Ni2-N5#4	174.6(3)
N6-Ni2-N5#4	94.1(3)	N4#4-Ni2-N5	91.2(2)
N4-Ni2-N5	81.8(2)	N6#4-Ni2-N5	94.1(3)
N6-Ni2-N5	174.6(3)	N5#4-Ni2-N5	90.8(3)

Symmetry transformations used to generate equivalent atoms: (#1) $-x + 1, -y, z$; (#2) $-x, -y, z$; (#3) $-x + 1, -y + 1, z$; (#4) $-x + 3/2, y, -z + 7/4$

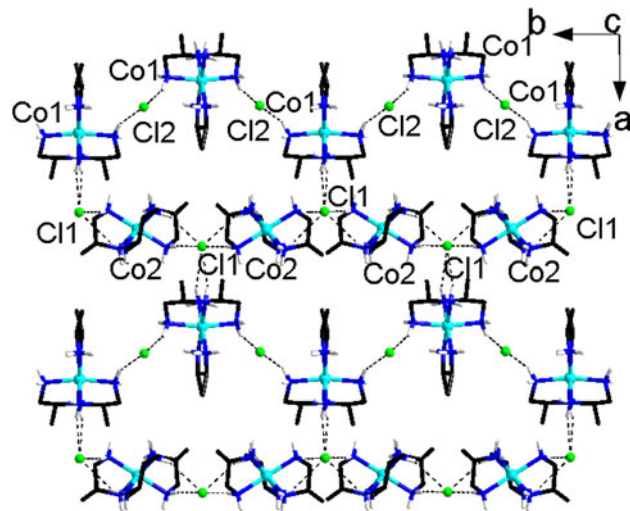


Fig. 2 Part of the crystal structure of **1**, showing the formation of a (100) sheet constructed from N–H...Cl H-bonds. H atoms bonded to C atoms are omitted for clarity

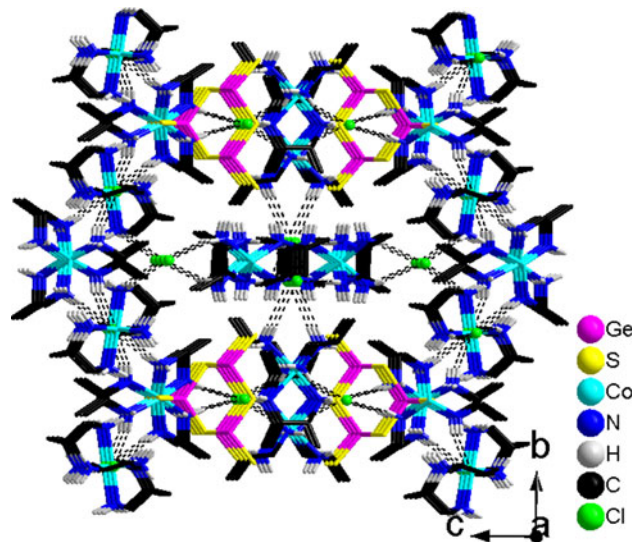


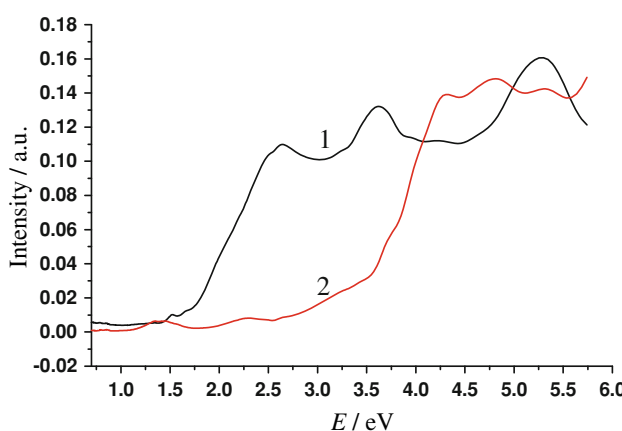
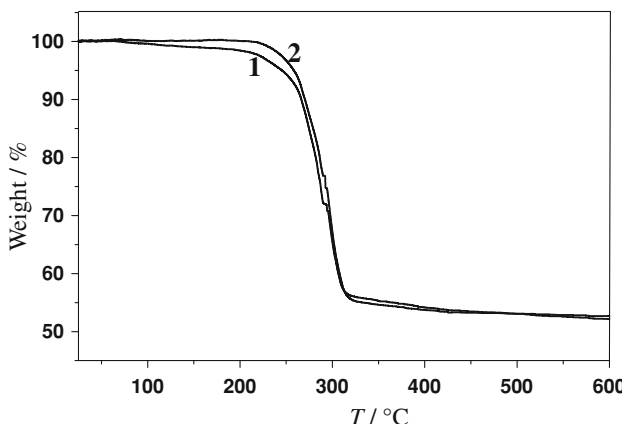
Fig. 3 3-D H-bonded network structure of **1**

Experimental

All chemicals were of analytical grade, and were obtained commercially and used without further purification. Fourier-transform infrared (FT-IR) spectra were recorded with a Nicolet Magna-IR 550 spectrometer in dry KBr pellets in the 400–4,000 cm^{-1} range. Elemental analysis was conducted with an EA-1110 elemental analyzer. UV–Vis spectra were recorded at room temperature using a computer-controlled PE Lambda 900 UV–Vis spectrometer.

Table 2 Hydrogen bonds for **1**

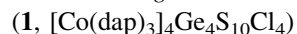
D-H...A	<i>d</i> (D-H) (Å)	<i>d</i> (H...A) (Å)	<i>d</i> (D...A) (Å)	$\angle(\text{DHA})$ (°)
N1-H1B...Cl1	0.90	2.80	3.665(5)	162.6
N2-H2A...S1#3	0.90	2.68	3.466(5)	145.8
N2-H2A...S2#1	0.90	2.87	3.574(5)	136.6
N2-H2B...Cl2	0.90	2.58	3.394(5)	151.6
N3-H3A...S2	0.90	2.90	3.715(7)	151.4
N5-H5A...Cl1#4	0.90	2.43	3.327(5)	174.6
Symmetry transformations used to generate equivalent atoms: (#1) $x, -y + 1/2, -z + 5/4$; (#2) $-x, -y, z$; (#3) $-x + 1, y + 1/2, -z + 5/4$; (#4) $x - 1, y, z$; (#5) $y - 1/2, x - 1/2, -z + 3/2$				
N5-H5B...S1#2	0.90	2.60	3.392(5)	148.0
N6-H6A...Cl2#5	0.90	2.57	3.440(5)	163.4
N6-H6B...S1	0.90	2.58	3.405(5)	153.4
N7-H7A...Cl1#4	0.90	2.86	3.663(6)	149.6
N7-H7B...S1	0.90	2.55	3.380(5)	153.2

**Fig. 4** Solid-state optical absorption spectra of **1** and **2****Fig. 5** TG curves of **1** and **2**

equipped with an integrating sphere in the wavelength range of 200–2,000 nm. Thermogravimetric analyses (TGA) were performed using a Mettler TGA/SDTA851 thermal analyzer under N₂ atmosphere with heating rate of 10 °C min⁻¹ in the temperature region of 25–600 °C.

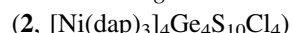
Powder X-ray diffraction (XRD) patterns were collected on a D/MAX-3C diffractometer using graphite-monochromatized Cu K_α radiation ($\lambda = 1.5406 \text{ \AA}$).

Tetrakis[tris(1,2-propanediamine)-cobalt(II)]-decathiotetragermanate tetrachloride



GeO₂ (0.0105 g, 0.1 mmol), 0.0160 g S (0.5 mmol), 0.0113 g Sb powder (0.1 mmol), 0.0237 g CoCl₂·6H₂O (0.1 mmol), and 2 cm³ dap were mixed in a thick-walled Pyrex tube. The sealed tube was heated at 170 °C for 6 days to yield yellow block crystals (31% yield based on GeO₂). IR: $\bar{\nu} = 3,252$ (m), 3,150 (m), 2,958 (m), 2,874 (m), 2,344 (w), 1,649 (w), 1,581 (vw), 1,455 (m), 1,397 (m), 1,011 (vw), 927 (w), 675 (s), 541 (m), 475 (s), 420 (m) cm⁻¹.

Tetrakis[tris(1,2-propanediamine)-nickel(II)]-decathiotetragermanate tetrachloride



Purple block crystals of **2** were prepared by a similar method used in the synthesis of the crystals of **1** except that CoCl₂·6H₂O was replaced by NiCl₂·6H₂O (43% yield based on GeO₂). IR: $\bar{\nu} = 3,244$ (m), 3,160 (m), 2,932 (m), 2,866 (w), 1,673 (w), 1,589 (m), 1,473 (m), 1,305 (w), 1,035 (vw), 649 (s), 557 (m), 473 (m), 423 (m), 418 (m) cm⁻¹. The experimental and simulated XRD patterns of **1** and **2** are shown in Fig. 6. The experimental peak positions are in agreement with simulated XRD pattern, indicating the phase purity of **1** and **2**. The difference in reflection intensity between experimental and simulated XRD patterns is probably due to the preferred orientation effect of the powder sample during collection of the experimental XRD data.

X-ray crystal structure determination

Data collection was performed on a Rigaku Mercury charge-coupled device (CCD) diffractometer with graphite-

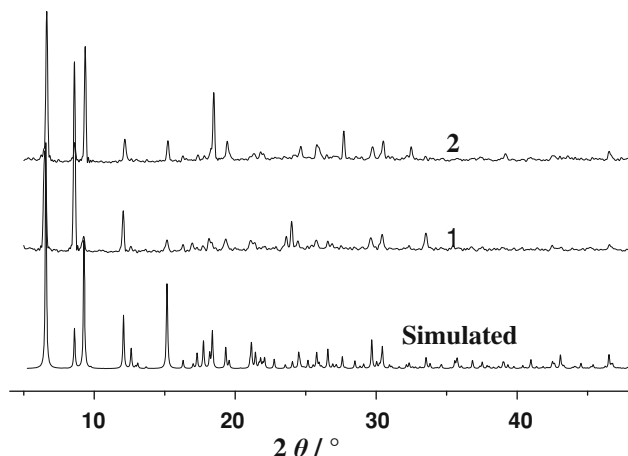


Fig. 6 Simulated and experimental powder XRD patterns of **1** and **2**

Table 3 Crystal structure data for **1** and **2**

	1	2
Formula	C ₃₆ H ₁₀₈ Cl ₄ Co ₄ Ge ₄ N ₂₄ S ₁₀	C ₃₆ H ₁₀₈ Cl ₄ Ge ₄ N ₂₄ Ni ₄ S ₁₀
FW	1,866.12	1,865.16
Crystal system	Tetragonal	Tetragonal
Space group	<i>I</i> 4 ₁ 2 ₂	<i>I</i> 4 ₁ 2 ₂
<i>a</i> (Å)	14.9185(18)	14.9235(12)
<i>b</i> (Å)	14.9185(18)	14.9235(12)
<i>c</i> (Å)	38.744(9)	38.725(7)
<i>V</i> (Å) ³	8,623(2)	8,624.5(18)
<i>Z</i>	4	4
<i>T</i> (K)	293(2)	293(2)
Calc. (density/ Mg m ⁻³)	1.438	1.436
Abs (coeff/ mm ⁻¹)	2.530	2.634
<i>F</i> (000)	3,824	4,160
2 <i>θ</i> (max) (°)	50.20	50.18
Total reflns collected	22,980	23,484
Unique reflns	3,845	3,851
No. of param	198	198
<i>R</i> 1 [<i>I</i> > 2σ(<i>I</i>)]	0.0420	0.0438
<i>wR</i> 2 (all data)	0.1278	0.1177
GOF on <i>F</i> ²	1.046	1.048
Peak and hole/ e (Å ⁻³)	0.886 and -0.472	0.518 and -0.371

monochromated Mo K_α radiation ($\lambda = 0.071073$ nm) at 293(2) K with maximum 2θ value of 50.20°. The intensities were corrected for Lorentz and polarization effects. The structures were solved with direct methods using the SHELXS-97 program [28], and refinement was performed against F^2 using SHELXL-97 [29]. All nonhydrogen atoms

were refined anisotropically. The H atoms of the organic amines, except for the C5 and C10 atoms, were positioned with idealized geometry and refined with fixed isotropic displacement parameters. C4 and C9 atoms were disordered over two positions with occupation ratio of 0.50:0.50. Relevant crystal and collection data parameters and refinement results can be found in Table 3.

CCDC 801457 (**1**) and 801458 (**2**) contain the supplementary crystallographic data for this paper. These data can be obtained free of charge from the Cambridge Crystallographic Data Centre via http://www.ccdc.cam.ac.uk/data_request/cif [or from the Cambridge Crystallographic Data Centre, 12, Union Road, Cambridge CB2 1EZ, UK; fax: (international) +44-1223-336033; e-mail: deposit@ccdc.cam.ac.uk].

Acknowledgments This work was supported by the NNSF of Chain (grant 20961011), China Postdoctoral Science Foundation (grant 20090450183), the NSF of Guangxi Province (grant 2010GXNSFB013017), and the NSF of the Education Committee of Guangxi Province (grant 201012MS182). The authors are also grateful to Yulin Normal University for financial support.

References

1. Armatas GS, Kanatzidis MG (2009) *Nat Mater* 8:217
2. Liao JH, Marking GM, Hsu KF, Matsushita Y, Ewbank MD, Borwick R, Cunningham P, Rosker MJ, Kanatzidis MG (2003) *J Am Chem Soc* 125:9484
3. Tampier M, Johrendt D (2001) *Z Anorg Allg Chem* 627:312
4. McGuire MA, Reynolds TK, DiSalvo F (2005) *J Chem Mater* 17:2875
5. Tan K, Ko Y, Parise JB, Darovsky A (1996) *Chem Mater* 8:448
6. Bowes CL, Huynh WU, Kirkby SJ, Malek A, Ozin GA, Petrov S, Twardowski M, Young D (1996) *Chem Mater* 8:2147
7. Cahill CL, Parise JB (1997) *Chem Mater* 9:807
8. Bonhomme F, Kanatzidis MG (1998) *Chem Mater* 10:1153
9. Cahill CL, Ko Y, Hanson JC, Tan K, Parise JB (1998) *Chem Mater* 10:1453
10. Tan K, Darovsky A, Parise JB (1995) *J Am Chem Soc* 117:7039
11. Zhang Q, Bu X, Lin Z, Biasini M, Beyermann WP, Feng P (2007) *Inorg Chem* 46:7262
12. Zhou J, Yin X, Zhang F (2010) *Inorg Chem* 49:9671
13. Zhou J, Dai J, Bian G, Li C (2009) *Coord Chem Rev* 253:1221
14. Stephan H, Kanatzidis MG (1997) *Inorg Chem* 36:6050
15. Vaqueiro P, Darlow DP, Powell AV, Chippindale AM (2004) *Solid State Ionics* 172:601
16. Vaqueiro P, Chippindale AM, Powell AV (2004) *Inorg Chem* 43:7963
17. Stephan H, Kanatzidis MG (1996) *J Am Chem Soc* 118:12226
18. Lühmann H, Rejai Z, Möller K, Leisner P, Ordolff M, Näther C, Bensch W (2008) *Z Anorg Allg Chem* 634:1687
19. Kiebach R, Bensch W, Hoffmann R, Pöttgen R (2003) *Z Anorg Allg Chem* 629:532
20. Kiebach R, Studt F, Näther C, Bensch W (2004) *Eur J Inorg Chem* 2553
21. Jia D, Dai J, Zhu Q, Cao L, Lin H (2005) *J Solid State Chem* 178:874
22. Chen J, Jin Q, Pan Y, Zhang Y, Jia D (2010) *Z Anorg Allg Chem* 636:230

23. Liu G, Guo G, Wang M, Cai L, Huang J (2010) *J Mol Struct* 983:104
24. Zhou J, Bian G, Zhang Y, Dai J, Cheng N (2007) *Z Anorg Allg Chem* 633:2701
25. Zhou J, Fang W, Rong C, Yang G (2010) *Chem Eur J* 16:4852
26. Zheng N, Bu X, Feng P (2005) *Chem Commun* 2805
27. Rothenberger A, Shafeei-Fallah M, Kanatzidis MG (2010) *Inorg Chem* 49:9749
28. Sheldrick GM (1997) SHELXS-97, Program for the Solution of Crystal Structures, University of Göttingen, Göttingen, Germany. See also: Sheldrick GM (1990) *Acta Crystallogr A* 46:467
29. Sheldrick GM (1997) SHELXL-97, Program for the Refinement of Crystal Structures, University of Göttingen, Göttingen, Germany. See also: Sheldrick GM (2008) *Acta Crystallogr A* 64:112